Second Transfer Process Simulation II

Toyoshige Sasaki[1], Kousuke Yamamoto[1], Takuma Onishi[1], Asako Sugiyama[1], Takeshi Tomizawa[2], Yasuo Yoda[3]
**1 Analysis Technology Center, Canon Inc., Tokyo, Japan*
**2 Office Imaging Products Device Development Center, Canon Inc., Ibaraki, Japan*
**3 Peripherals Development Center, Canon Inc., Shizuoka, Japan*

Abstract

In the second transfer process, electrostatic forces, caused by the transfer electric field, act on a sheet in the nipped region. As a result, the sheet sticks to the roller, and sheet transportation fails. We have developed a numerical simulation method of sheet transportation in the second transfer process. The method calculates sheet transportation by means of weak-coupling between electric field analysis and structural analysis, and which considers electrostatic forces acting on the sheet and displacement of components relative to each other. We used the method to calculate sheet transportation in a system that consists of two rollers and the sheet between them. In this system, the sheet passes between two rollers which contact each other and to which a voltage is applied. The calculated charge density and sheet displacement showed good agreement with experiments. Another analysis clarified the relationship between electric discharges in the nipped region and sheet sticking to the roller.

Introduction

One of the problems that may occur in the second transfer process is that a sheet winds around a roller. Electrostatic forces caused by the electric field in the transfer area act on the sheet as it passes through the nipped region, because the sheet has electric charge. These forces may cause the sheet to wind around a roller and result in defective transportation. One study has studied the electrostatic forces operating on the sheet by calculating the electric field analysis. With this result, it developed a structural analysis and calculated sheet deformation[1]. However, the sheet deformation depends on the electric charges of the sheet influenced by the deformation of the sheet. Therefore, we must consider both the electric charges and the deformation of the sheet in order to calculate sheet transportation precisely.

In this study, we developed a numerical simulation method, assessed its reliability, and clarified the mechanism by which a sheet sticks to a roller.

Simulation Method

Calculation Flow

We developed a program to calculate sheet transportation, and Figure 1 illustrates a flowchart of the program. This program weak-couples the electric field analysis and structural analysis based on the finite element method.

1. The program reads two finite element models(FE models): one for the electric field analysis and the other for the structural analysis. Each FE model is shown in Figure 2. In the electric field analysis, the air area needs to be divided into every element. The elements near the nipped region need to be divided more finely in order to consider the electric discharges at the microgap. Therefore, two different FE models are used for the electric field analysis and structural analysis.

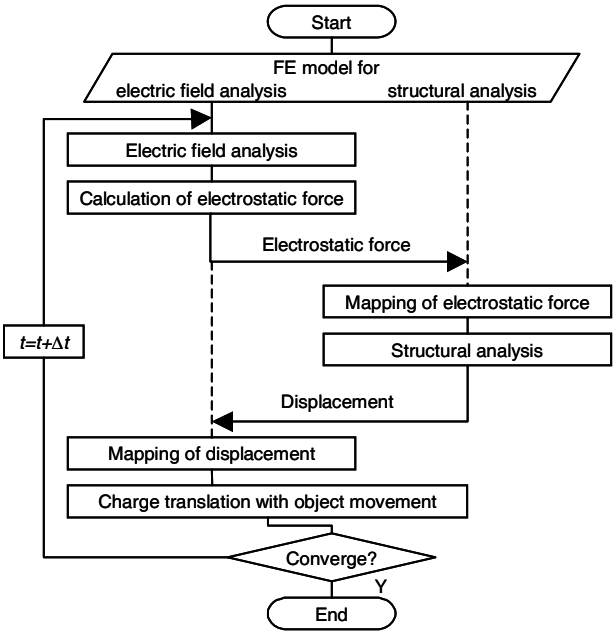

***Figure 1**. Simulation flowchart*

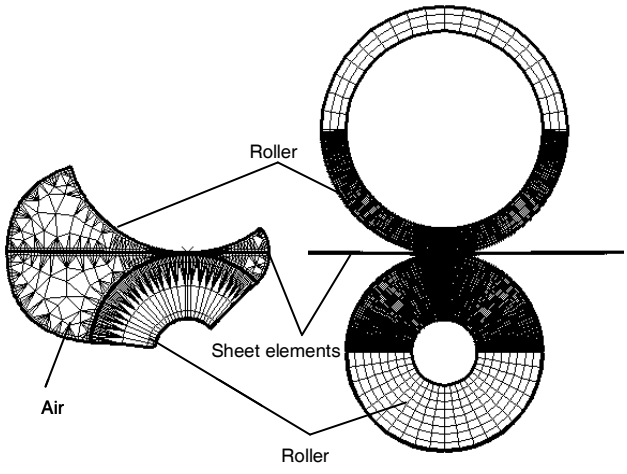

***Figure 2**. The simulation FE models*

2. The electric field analysis is performed taking into consideration electric conduction and electric discharge. This makes it possible to calculate the distribution of the electric charge and electric field [2].

3. The program calculates the electrostatic force F acting on a sheet by using the equation [1]:

$$F = (\sigma_A + \sigma_B)\frac{E_\alpha + E_\beta}{2} \quad (1)$$

where σ_A, σ_B, E_α and E_β are the surface charge densities on the obverse of the sheet, the reverse of the sheet, the electric field on the obverse of the sheet, and the electric field on the reverse of the sheet, respectively. Eq. (1) is applied to each node on the sheet surface in the FE model for the electric field analysis to calculate the distribution of electrostatic forces acting on the sheet.

4. The program maps the electrostatic forces. Electrostatic forces calculated for the nodes composing the sheet in the FE model for the electric field analysis by using Eq. (1) are transformed into those of the nodes composing the sheet in the FE model for the structural analysis.

5. The program performs the structural analysis in consideration of the electrostatic forces acting on the sheet to calculate the displacement of the nodes in components.

6. The program maps the displacement as follows. The displacement of nodes in the FE model for the structural analysis is transformed into that of nodes in the FE model for the electric field analysis. The nodes in the FE model for the electric field analysis move according to the displacement. In addition, the nodes of the air area also move according to the deformation of components as crushing elements do not form.

7. The program transfers charge on the surface of the object as the object advances.

The program performs the electric field analysis by using the FE model for the electric field analysis after deformation and repeat the procedure described above.

Sheet Transportation

As shown in Figure 2, sheet elements must be prepared over the entire range of the analysis area in each FE model. In each calculation process, the following calculations are carried out, according to the arrival position of the sheet at each time step.

In the electric field analysis, the material properties of air are applied where the sheet does not reach. The material properties of the sheet itself are applied where the sheet reaches.

On the other hand, in the structural analysis, the sheet exists over the entire range of the analysis area, and therefore the sheet is not transferred during this process. A static calculation of deformation is executed assuming that two rollers pinch the sheet in each time step. This is based on the experience that there is little difference between actual sheet transportation and this static analysis.

This method allows to model sheet transportation.

Results and Discussion

Analysis Model

Figure 3 shows the system for sheet transportation. Roller B is kept pressed against Roller A. A sheet is inserted between the two rollers and is transferred as Roller A rotates. Roller A is made of metal, and its diameter is 30mm. Roller B is made of rubber, and we use five kinds of rollers having different diameters. Both Roller A and B are 8cm long. The load applied to Roller B is 1 kgf, and the voltage is applied to the shaft of Roller B. A PET film is used as the sheet, and it moves at 130mm/sec. The material properties of each component are shown in Table 1.

The PET film is charged only by electric discharges, since PET is an insulator. The PET film accumulates negative charge by receiving electric discharges from Roller A and accumulates positive charge by receiving electric discharges from Roller B. The electric charges on the PET film are given by the sum of the charges on both sides of the film.

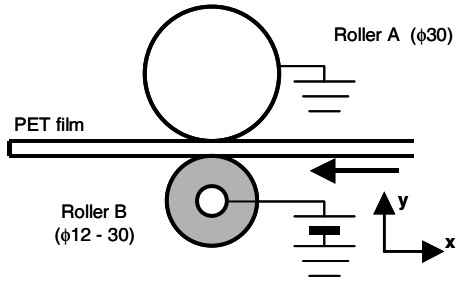

***Figure 3**. The test model*

Table 1 Material properties

	Roller A	Roller B	PET
Conductivity [S/m]	∞	3.0×10^{-7}	0
Permittivity	-	10	3
Young's Modulus [MPa]	5000	3.0	4000
Poisson's Ratio	0.35	0.49	0.3

Charge on PET Film

We transferred a 100μm thick PET film while applying 3 kV to Roller B, and measured the charge density on the PET film as follows. We set the PET film after transportation on a grounded electrode, measured its surface potential, and converted it into charge density. The reason for using a 100μm thick PET film is to prevent the film from winding around the rollers, and this allows measuring the surface potential easily.

The experimental and calculation results are shown in Figure 4, revealing relationship between the decrease of charge density and the increase of diameter of Roller B.

Sheet Deformation

We transferred a 50μm thick PET film while applying 2 kV to Roller B and studied the deformation of the PET film. Figure 5 shows the condition of transportation associated with the change of D, which is the sheet length from the center of the nipped region to the tip of the sheet. The roller B diameter is 20mm. Figure 5(a) shows the experimental results, and Figure 5(b) shows the calculation results, where contours and arrows are electric potential distribution and electrostatic forces acting on the sheet, respectively. Figure 5(c), a close-up of the nipped region from the calculation results, shows the condition of electric discharges.

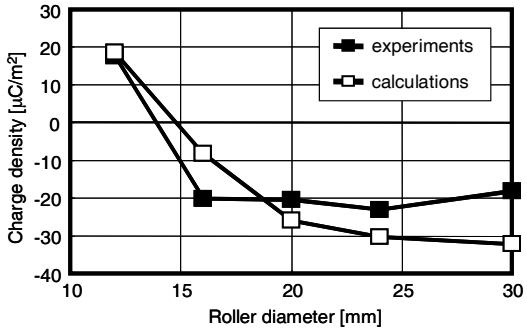

***Figure 4**. Relationship between the roller diameter and charge density on PET*

In Figure 5(b), the PET film, after passing the nipped region, winds around Roller A. This shows good agreement with the experiment in Figure 5(a). The phenomenon is explained chronologically based on the calculation results. At D = –2mm, the PET's tip is not reached the nipped region. Thus, Roller A and B are in a state of conduction with each other. At D = 1mm, the PET's tip slightly passes the nipped region. In the upper nipped region, the PET film receives electric discharges on both surfaces. The direction of the electrostatic force acting on the PET film is acting toward Roller A, as the total electric charge is positive. On the contrary, in the lower nipped region, the direction of the electrostatic force is acting toward Roller B, as the negative electric discharges are stronger while the PET film receiving electric discharges on both surfaces. At D = 4mm, the part with positive charge in the upper nipped region reaches the lower region. The PET film is still transferred straight. At D = 7mm, the PET film begins to stick to Roller A as the part with positive charge in the upper nipped region passes through the lower region. Consequently, the air gap between Roller A and the PET film disappears, and it vanishes electric discharges in the area. This means that electric discharges in the lower nipped region are only positive at this time. As a result, the sticking area extends rapidly until the sheet reaches D = 10mm.

Figure 6 compares the trajectories of the PET's tip between the experiment and calculation for various diameters of Roller B. Coordinate axes are defined as shown in Figure 3, and the origin exists at the center of the nipped region. The calculation results and experimental results show the same tendency in the following respect. The sheet winds around Roller A at the roller diameter of 12mm, but tends to wind around Roller B for the larger diameter of Roller B. This occurs because the negative discharges from Roller A in both the upper and lower nipped regions become more dominant with the larger roller diameter. The calculation results agree with the experimental ones for Roller B at 12mm or 20mm, but do not agree at 24mm or 30mm. This is probably because the phenomena occurring during the transition in sticking direction are very delicate.

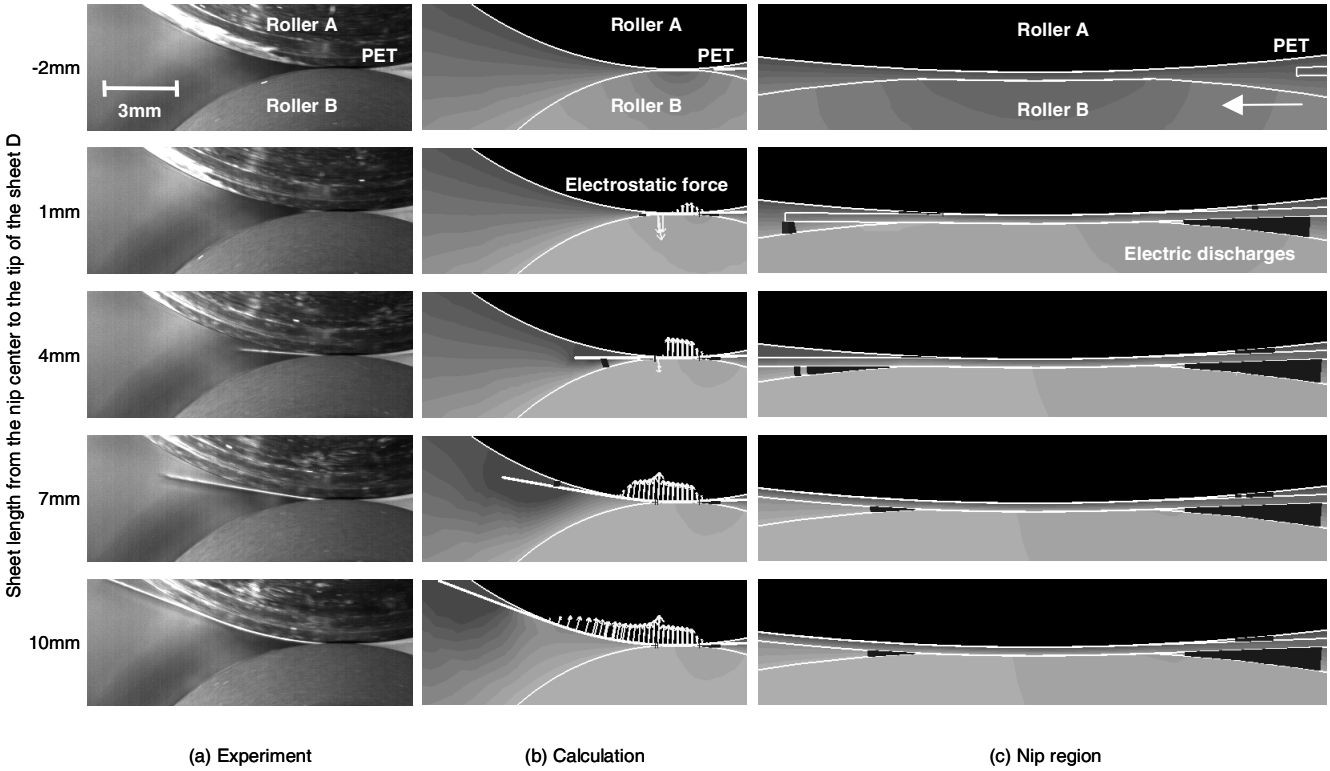

***Figure 5**. Comparison of PET transportation*

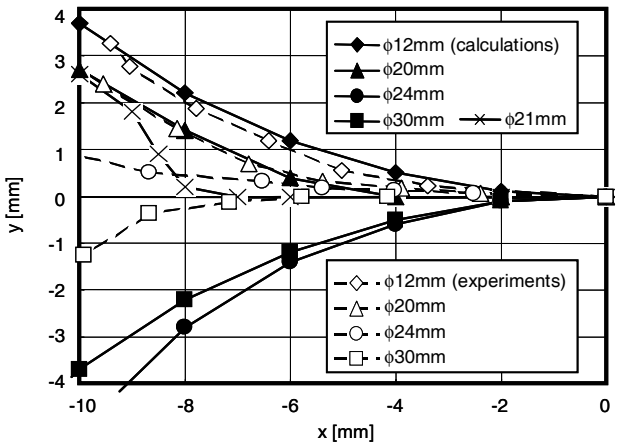

***Figure 6**. Trajectory of PET tip*

Sheet Sticking

The experimental result for the 30mm roller in Figure 6 shows that the PET film winds around Roller B rapidly after it is transferred nearly straight to the position x = –8mm. This phenomenon often occurs in the development phase of the transfer process. Since this phenomenon is very noticeable in the calculation result for the 21mm roller as shown in Figure 6, we came to the realization that we must analyze the causes and effects.

Figure 7 shows the transition of the condition in the lower nipped region for the 21mm roller. Figure 7(a) shows the sheet deformation, and Figure 7(b) compares the change of the electric field between Roller A and the PET film(E_{gap}) with the Paschen's electric field($E_{pa} = V_{pa}$/gap). The condition of the PET film at each position is as follows. At D = 4mm, the part with positive charge in the upper nipped region reaches the lower region. At D = 7.4mm, the PET film is right before beginning to wind rapidly. At D = 8.3mm, the PET film is winding. The electric field distribution in Figure 7(a) shows that the gap between Roller A and the PET film at D = 7.4mm is slightly shorter than that at D = 4mm. Although the electric discharges decrease, they still occur over a wide area. The electric field curve slightly moves in parallel toward the negative direction of the x-axis because of the gap decrease as shown in Figure 7(b). In addition, at D = 8.3mm, the curves of the electric field at the gap and the Paschen's electric field separate from each other as shown in Figure 7(b), and the electric discharges between Roller A and the PET film disappear. The electric discharges occurring in the lower nipped region disappear rapidly as the gradient of the electric field curve nearly equals that of the Paschen's curve. Therefore, the cause of the PET film winding rapidly is instantaneous disappearance of the negative electric discharges from Roller A.

Conclusion

We developed a method of calculating sheet transportation in the second transfer process by means of weak-coupling between electric field analysis and structural analysis by transmitting electrostatic forces and displacements between each other.

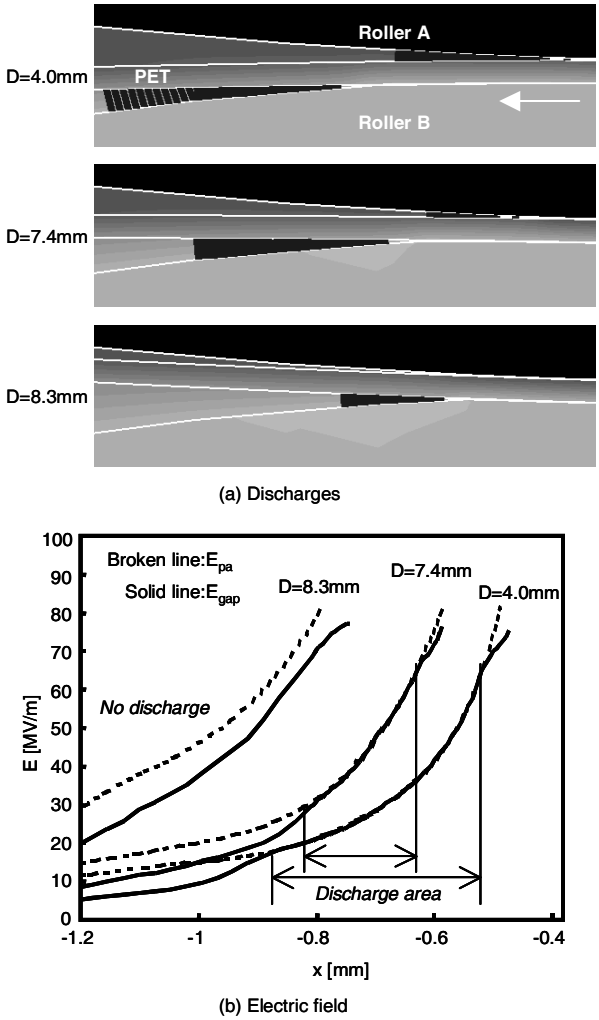

***Figure 7**. Electric discharges and electric field in the lower nipped region*

We used the method to calculate the transportation of a PET film, and the results qualitatively agreed with those of experiments. Further, we clarified the relationship between electric discharges in the nipped region and sheet deformation.

References

[1] T. Nagao, Z. Li, N. Nakayama, Analysis of paper deformation in electrophotography transfer process, Proc. Japan Hardcopy 2000 Fall Meeting, pg. 53 (2003).

[2] T. Sasaki, T. Onishi, A. Sugiyama, Y. Yoda, T. Tomizawa, Second Transfer Process Simulation I, Proc. IS&T's: NIP24 (2008).

Author Biography

Toyoshige Sasaki received his B.S. and M.S. degrees from Waseda University, Japan in 1982 and 1984, respectively. He joined Canon in 1984 and has been engaged in the development of electromagnetic devices such as magnetic recording media, actuators, and electro-photography by using numerical simulation.